ACS APPLIED MATERIALS & INTERFACES

RESEARCH ARTICLE

www.acsami.org

Increasing Surface Area of Silica Nanoparticles With a Rough Surface

Shuping Xu, Shay Hartvickson, and Julia Xiaojun Zhao*

Department of Chemistry, University of North Dakota, Grand Forks, North Dakota 58202, United States

Supporting Information

ABSTRACT: The silica nanoparticles with a rough surface were developed using a silane precursor in a reverse microemulsion followed by a drying treatment. The surface roughness of the nanoparticles was adjustable by changing the amount of the precursor. Within a certain range, the roughness increased as the amount of the silane precursor increased. The rough surface provided a larger surface area than the smooth one. The produced nanoparticles were characterized using the transmission electron microscopy, ultraviolet−visible spectroscopy, energy-dispersive X-ray elemental analysis, and Brunauer−Emmet−Teller analysis technique. Additionally, the amount of surface functional amino groups on the nanoparticles was detected using the traditional acid−base titration and the dissociation constant of this functional group was calculated. On the basis of the experimental results, the mechanism of the formation of the rough surface was proposed. Finally, the produced silica nanoparticles were utilized as a carrier for the chemical binding of a near-infrared dye molecule and the adsorption of the gold nanoparticles. The results demonstrated that the rough surface provide the silica nanoparticles with a high capacity of surface chemical and supramolecular reactions.

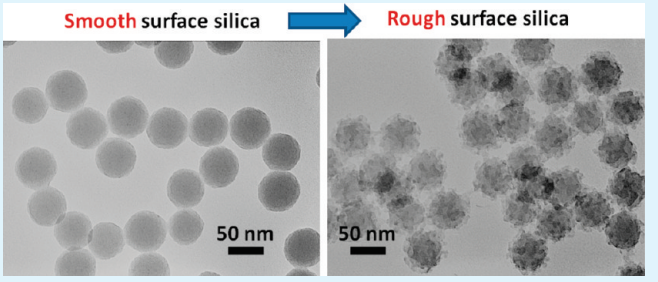

KEYWORDS: silica nanoparticles, rough surface, surface modification, APTS, nanocomplex

1. INTRODUCTION

Silica nanomaterials have a broad range of applications due to their unique features: little absorption in the ultraviolet−visible (UV−vis) and near-infrared (NIR) regions, dielectric electrons, and low toxicity.[1−4] These features allow the silica nanoparticles to be widely utilized as the solid-supporting or entrapping matrix.[5−9] Compared with other inherently functional nanomaterials (e.g., semiconductor quantum dots, carbon nanotubes, plasmonic nanoparticles, and magnetic nanoparticles), the merits of silica nanoparticles could be totally embodied in their applications only when combined with other materials with remarkably optical, magnetic, electrical, catalytic, or biological properties.[10−17] These functional materials can be either encapsulated inside the silica matrix or linked to the surface of the silica nanoparticles. The latter pathway will need functional sites on the silica nanoparticle surface to link the functional molecules. On this pathway, to achieve a broad range and a high efficiency of applications, a large amount of surface functional sites on the nanoparticles are needed.

There are two main methods for the preparation of silica nanoparticles: the Stöber sol−gel method[18] and the water in oil (w/o) reverse microemulsion method.[19] Both methods are based on the hydrolization and condensation of tetraethylorthosilicate (TEOS) under the acidic or basic conditions. Using these two methods, the most-produced silica nanoparticles are perfect spheres (or a few ellipsoids) with a smooth surface covered by hydroxyl groups. However, the hydroxyl group is too limited to cope with the requirements of various linking reactions. Thus, further surface functionalization is needed to provide a diverse range of chemical groups to make the silica nanoparticles accessible to various surface linking strategies. Meanwhile, a smooth surface provides limited surface area as the size of nanoparticles is fixed. For a required dimension, a possible way to increase the surface area is to make nanoparticles with a rough surface.

The morphological changes can directly alter the properties of nanomaterials, including the physical constants (density, surface area, porosity, etc.), optical properties,[20] and wetting behaviors.[21,22] Thus, in addition to the increased surface area, the rough surface will provide the functional materials with different binding capacity because the immobilization of many functional molecules are based on the selective adsorption interaction,[23−25] such as catalysts, enzymes, antibodies, and drugs. It has been reported that the adsorption kinetics on a rough surface is different from that on a smooth surface because of the different diffusion rate through a stagnant layer of solvent near the surface.[26] The slow chemical reaction of the encapsulated functional molecules with the outside targets has been reported for the silica-based nanoparticles.[27] The rough surface may speed up this reaction through an easier surface adsorption of targets. Thus, the silica nanoparticles with a rough surface may advance the applications of silica-based nanomaterials.

So far, several physical methods have been developed to prepare the rough or pattern surfaces, such as nanosphere lithography,[28] electron-beam lithography,[29] and optical lithography.[30] These methods are usually carried out on flat substrates. It is difficult to

Received: January 14, 2011
Accepted: May 11, 2011
Published: May 11, 2011

perform these techniques on a curved surface, even the architecture on a single spherical nanoparticle. Thus, the current physical methods are not applicable for making silica nanoparticles with a rough surface. A chemistry approach might be considered. For a chemical reaction in a solution, all dimensions of the nanoparticle surface are accessible for manipulation of surface roughness. Meanwhile, considering the facile treatment process and the relatively low cost of the equipment required, a chemical approach is preferred for manipulating silica nanoparticles.

Recently, it has been found that several organotriethoxysilane precursors could lead to the mesoporous silica particles when co-condensing with TEOS in a micelle-forming surfactant system.[31] The silane precursors have been used for modification and functionalization of silica nanoparticles through postcoating of the silica nanoparticles. These precursors have similar structures to TEOS and share the same mechanism of hydrolization and condensation. Differing from TEOS, these silane precursors provide multifunctional groups, for instance, mercapto, carboxyl, amino, and phosphonate, which increase the flexibility of surface reactions and extend the applied fields of silica nanoparticles.[14−17,23,24] Different silane precursors co-condensing with TEOS not only alter the distribution of the functional groups on the silica nanoparticle surface, but also may change the morphology of the silica matrix. However, so far, the effect of the silane precursors on the morphology of the produced silica nanoparticles has been rarely discussed in the literature.

In this study, we aimed to develop a chemical method for making rough surface of silica nanoparticles. Furthermore, the roughness of this nanoparticle could be manipulated by simply changing the synthetic conditions. To understand the chemistry behind this phenomenon, a mechanism of forming a rough surface was proposed. Finally, the applications of the rough surface were demonstrated by both chemical and supramolecular surface reactions. This work should provide new insights into the manipulation of silica surface for advancing applications of the silica-based nanomaterials.

2. EXPERIMENTAL SECTION

2.1. Chemical Reagents. Tetraethylorthosilicate (TEOS, 98%, 0.94 g/mL, MW = 221.37) and methyl sulfoxide (DMSO) were purchased from Acros Organics. 3-Aminopropyltriethoxysilane (APTS, 95%), 3-mercaptopropyltrimethoxysilane (MPTS), polyoxyethylene(10) isooctylphenylether [Triton X-100, 4-(C_8H_{17})C_6H_4(OCH_2CH_3)$_{10}$−OH], and 1′-bis(4-sulfobutyl)-11-(4-isothiocyanatophenylthio)−3,3,3′,3′-tetramethyl-10,12-trimethyleneindotricarbocyanine monosodium salt (NIR 797 isothio-cyanate, MW = 880.14, 75% HPLC, Fluka Chemie) were purchased from Sigma-Aldrich Inc. Ammonia (29.5%, ACS) and cyclohexane (HPLC grade) were purchased from Fisher Scientific. 1-Hexanol (99+%) was purchased from Alfa Aesar. Milli-Q water (18.6 Ω cm^{-1}) has been used to make aqueous solution.

2.2. Preparation of Silica Particles with a Loose Shell and Rough Surface. Silica nanoparticles were synthesized using a reverse microemulsion method.[6] Briefly, 7.50 mL of cyclohexane was used as the organic solvent. A 1.77 mL aliquot of Triton X-100 as the surfactant and 1.80 mL of 1-hexanol as the cosurfactant were both added into the stirring cyclohexane. Then, 480 μL of water was added into the mixture solution. The water was totally dispersed into cyclohexane since they formed droplets in the presence of surfactants (Triton X-100 and 1-hexanol). Afterward, 50 μL of TEOS was added into this microemulsion followed by 60 μL of ammonia to catalyze the hydrolization of TEOS to form compact silica cores. After stirring 24 h, a 50 μL aliquot of TEOS and varying amounts of APTS were added to the above mixture for the postcoating treatment. The TEOS and APTS were allowed to hydrolyze under stirring for another 24 h. In this process, the hydrolyzed TEOS and APTS were deposited onto the silica cores and formed a layer of silica shell.

The microemulsion was broken by adding 20 mL of acetone. The silica nanoparticles were separated from the supernatant by centrifugation and were washed with a large amount of ethanol three times. Finally, the silica precipitates were dried in air over two days. This drying treatment was a crucial step because the silica shell changed its density in this process and lead to different morphologies as the amount of APTS varied. The dried particles were grounded into fine powder before usage. Nanoparticle solutions were prepared by suspending the particulate powders into water and sonicating them for at least one hour. Usually, a 1.0 mg/mL nanoparticle solution was prepared as a stock solution.

2.3. Silica−NIR Dye Nanocomplex. NIR 797 isothiocyanate is a NIR fluorescent molecule. It can react with the amino groups on the nanoparticles by forming the covalent bonds under a mild alkaline condition (pH 8.0). A 10 μL aliquot of NIR 797 isothiocyanate in DMSO (10.0 mg/mL) The solution was kept at 4 °C overnight while the silica particles turned into dark green. The silica−NIR dye nanocomplexes were separated from solution by centrifugation and were washed three times with water. These colored precipitates were then diluted into water to form 1.0 mg/mL stock solutions.

2.4. Silica−Au Satellitic Nanocomplex. The Au-nanoparticles of 4 ± 1 nm in diameter were synthesized based on the literature method.[32] The silica nanoparticles were added into the gold nanoparticle solution and reacted for 5 min. The mixture was centrifuged at a speed of 3214 g. The excessive gold nanoparticles were in the supernatant and thus were removed. The silica−Au satellitic nanocomplexes were harvested from the precipitate.

2.5. Characteristics. *Size and Morphology.* The size and morphology of the silica nanoparticles were characterized using the transmission electron microscopy (TEM). A Hitachi 7500 TEM was used operating at 80 kV. The size of silica nanoparticles was obtained by measuring over 200 nanoparticles on the TEM images.

Surface Area. The specific surface area of the nanoparticles was measured by the Analytical Service Division at the Porous Materials, Inc. (Ithaca, NY). A PMI BET Sorptometer was employed for this measurement. About 100 mg of particle powder was used for each test. The testing temperature was −195.76 °C, and the adsorbent was nitrogen.

Adsorption Ability. The UV−vis spectra of the nanoparticles were obtained using a Shimadzu-4500 UV−vis spectrophotometer. The silica−NIR 797 isothiocyanate nanocomplex solution was sonicated until it was transferred into a 1 cm quartz cuvette for testing. The stock solution of nanoparticles was diluted by three times before the measurement. The concentration of silica nanoparticles was 0.33 mg/mL. The integral area of the absorption peak of NIR 797 isothiocyanate was measured for evaluation of the adsorption ability of different silica nanoparticles. The Origin 6.0 software was used for the calculation of the integral areas of the UV−vis spectra.

Elemental Analysis of the Nanoparticles. Elemental compositions of the developed nanoparticles were determined using energy-dispersive X-ray spectroscopy (EDS). An EDS detector was attached on a scanning electron microscope (SEM, Hitachi S3400N). SEM images were taken with an operating potential of 15 kV, along with the elemental analysis. Average values of 20 spots in an image were reported.

Amount of Amino Groups on the Nanoparticle Surface. The amount of amino groups on the nanoparticle surface was measured using a traditional acid−base titration. First, 1 mL of NaOH (0.0994 ± 0.0003 M) was added into 20 mL of nanoparticle aqueous solution containing 5.0 mg of the nanoparticles. This strong base could convert the $-NH_3^+$ to $-NH_2$. Under stirring, several microliters of HCl were added into the solution. The pH values were recorded and the titration

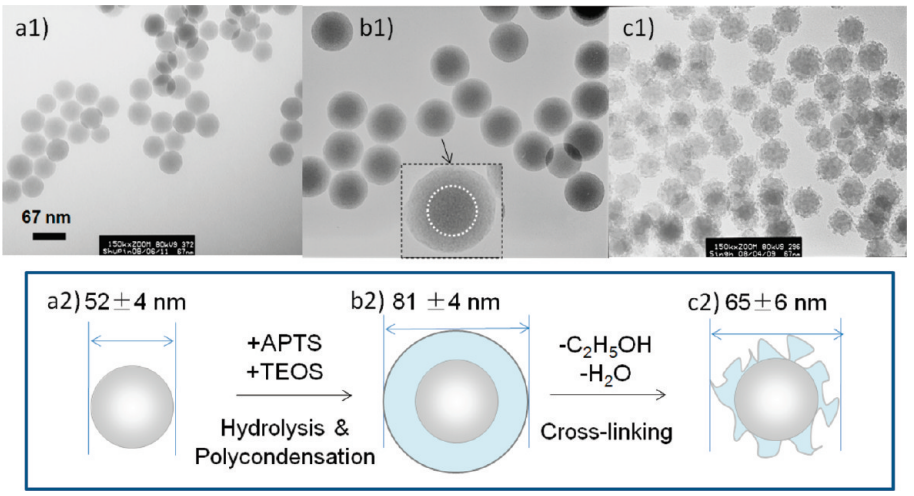

Figure 1. TEM images of silica nanoparticles. (a1) Core of pure silica nanoparticles; (b1) core−shell silica nanoparticles; (c1) dried nanoparticles in b1. (a2−c2) Schematic diagrams of the formation of the silica nanoparticle with a rough surface.

curve was plotted with the volume of HCl (0.104 ± 0.001 M). The HCl was standardized by dried Na_2CO_3 before use.

3. RESULTS AND DISCUSSION

3.1. Formation of Silica Nanoparticles with a Rough Surface. A w/o microemulsion is an isotropic and thermodynamically stable single-phase solution. Water droplets are formed in the bulk organic solvent and serve as nanoreactors for the synthesis of silica nanoparticles from various silane precursors. TEOS is a typical water-soluble precursor for the synthesis of silica nanoparticles. Upon the polymerization of TEOS, a silica core is formed within the water droplet. As the polymerization progresses, the silica core grows and finally a stable silica nanoparticle is produced in the water droplet.[8] In this work, the silica nanoparticles were produced using the protocol described in section 2.2.[8] They were all spherical in shape with the average diameter of 52 ± 4 nm (Figure 1, a1).

To modify the surface of the silica nanoparticles, we added additional TEOS and APTS (50 μL each) to the reverse microemulsion. The polymerization of these two precursors was allowed for 24 h. In this process, the hydrolyzed TEOS and APTS were codeposited onto the silica core and they formed a layer of silica shell. This shell presented less dense compared to the core, and thus was clearly identified from the enlarged nanoparticle on the TEM image (Figure 1, b1, the diameter of the core−shell nanoparticles was 81 ± 4 nm). The lighter gray indicated that the density of the shell was lower than that of the core.

An interesting new phenomenon was observed after we completely dried the produced core−shell silica nanoparticles for 2 days. The shell of silica nanoparticles was converted into a loose structure and the surface became significant rough. These morphology changes were clearly shown on the TEM image (Figure 1, c1). Compared to Figure 1 b1, it seemed that the completely drying treatment played an important role on the morphology change. In addition to this morphology change, after drying, the silica nanoparticles also shrank down to 65 ± 6 nm in diameter.

We have measured the dynamic size of three kinds of silica nanoparticles (Figure 1 a1, b1 and c1) with a dynamic light scattering (DLS) instrument (Malvern Nano ZS instrument). The results were shown in Supporting Information. The sizes of them in ethanol were 73.97, 98.86, and 84.33 nm, respectively.

The rough surface should provide the nanoparticle with a larger surface area than the smooth one. To learn the surface area change, Brunauer−Emmet−Teller (BET) analysis technique was used to measure the surface area of the silica nanoparticles. The results showed that the surface area of the nanoparticles was 81.2 m^2/g (see the Supporting Information). Theoretically, the smooth surface area of this sized silica nanoparticles is 47.0 m^2/g. The significant 72% increase of surface area was attributed to the morphology change of the nanoparticles. In fact, the BET technique measured the area from both the outer and inner locations and it could not clearly differentiate them. Because a loose layer of silica was produced, the increase in the surface area should include the contributions from both the outer and inner surfaces within this layer.

To summarize the morphology and size changes in the silica nanoparticle formation, a schematic diagram was shown in the bottom panel of Figure 1, in which a2, b2, and c2 corresponded to the images of a1, b1, and c1, respectively. The drying treatment seems to be the key process for the formation of such rough silica nanoparticles when APTS was used as the silane precursor.

3.2. Effect of the Amount of APTS on the Roughness of the Nanoparticles. To understand the function of APTS in the formation of the rough surface, we varied the amount of APTS but kept the amount of TEOS a constant value of 50 μL in the synthesis of the silica shell. All the nanoparticles experienced the drying treatment. Initially, without APTS, the silica nanoparticles possessed a smooth surface (Figure 2a). When 10 μL of APTS was added, the surface of the silica nanoparticles changed into an insignificant roughness (Figure 2b). When the amount of APTS was increased from 10 to 20, 30, and 40 μL, the roughness of the nanoparticle surface gradually increased (Figure 2c−e). The roughest surface was obtained when the amount of APTS increased to 50 μL (Figure 2f), which was equal to the amount of TEOS. These results clearly demonstrated that the APTS caused a rough surface and the extent of the roughness increased as the amount of APTS increased.

However, by the further increase in the APTS amount to 60 μL, the reverse microemulsion changed from a clear emulsion into a nontransparent mixture, and a great deal of white silica gel deposited on the walls of the reaction container. The size of the resultant

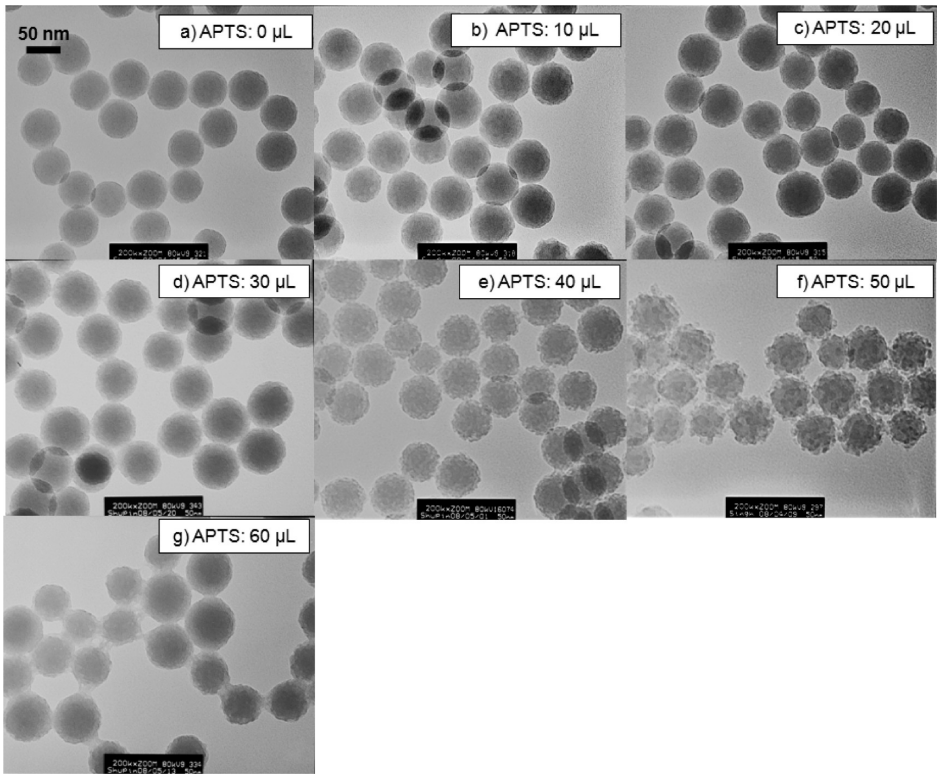

Figure 2. TEM images of the silica nanoparticles with different level of roughnes. Images a−g corresponded to the silica nanoparticles made by adding different amounts of APTS.

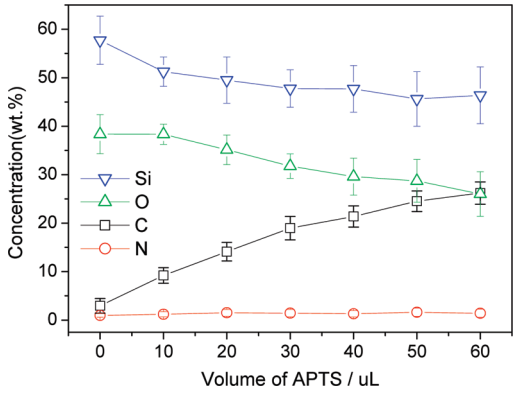

Figure 3. Elemental analysis of the developed silica nanoparticles using energy-dispersive X-ray spectroscopy.

nanoparticles was not uniform, and the rough surface significantly disappeared (Figure 2g). We have tested the APTS amount from 70 to 150 μL (not shown). All the TEM images of the produced silica nanoparticles showed similar morphologies to the products of the 60 μL-APTS trial. More silica gel appeared on the container wall as more APTS was used. The sedimentary silica gels indicated that the micelles in the reverse microemulsion have been destroyed. The micelles played an important role in the polymerization of silica precursor. The formation of the silica shell was limited within a micelle. When the micelles were destroyed, the growth of the silica shell was beyond control. It seemed that the majority of APTS was converted to silica gel. Thus, to obtain the roughest surface of silica nanoparticles, the selection of the optimum APTS amount is essential in addition to the drying treatment of nanoparticles.

3.3. Elemental Analysis of the Nanoparticles with a Rough Surface. The components of the resultant nanoparticles (Samples a−g in Figure 2) were analyzed using an EDS that was attached to a scanning electron microscope. The weight percentages of Si, O, C and N in different nanoparticles were shown in Figure 3. In the APTS free nanoparticles, the percentages of Si, O, C and N were 57.7, 38.3, 3.0, and 1.0%, respectively. As the APTS amount increased, the percentages of Si and O decreased; while the percentage of C increased remarkably. Corresponding to the APTS amount of 10, 20, 30, 40, and 50 μL, the carbon percentage was 9.2, 14.1, 19.0, 21.4, and 24.6%, respectively. The percentage of the nitrogen was suspect because their concentration was in the instrumental error range. There were two possible resources for increasing carbon: (1) the propyl group ($-C_3H_6-$) on the APTS molecule; (2) the possible unhydrolyzed oxyethyl groups ($-OC_2H_5$) from either TEOS or APTS. In the postcoating process, we only adjusted the amount of APTS and kept the TEOS amount in 50 μL for all trails. If there was any unhydrolyzed oxyethyl groups ($-OC_2H_5$) from TEOS, it should be consistent. The incremental changes on the carbon weight were only from the propyl and oxyethyl groups of the additional APTS. Thus, the EDS results demonstrated that a significant amount of APTS has successfully participated in the formation of the silica shell, and the amount of final deposited APTS could be directly altered by the amount of APTS added in the synthesis process. The elemental analysis results support that the APTS is indeed the key factor for forming the rough surface and the level of roughness is adjusted by changing the APTS amount.

3.4. Effect of a Similar Silane Precursor to APTS on the Formation of the Rough Surface. To investigate the effect of the chemical structure of the silane precursor on the formation of smooth or rough surfaces of silica nanoparticles, we used an additional silane precursor, MPTS, for the synthesis of the silica

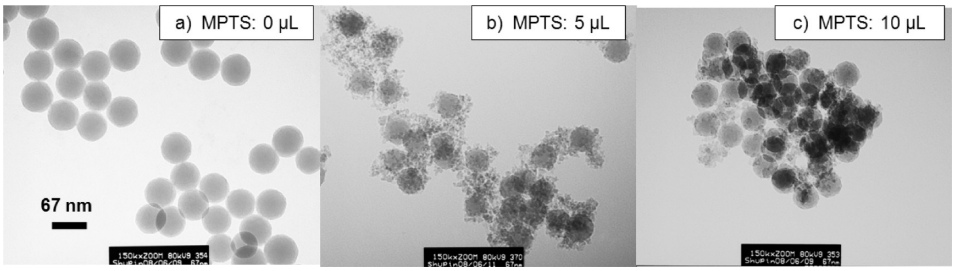

Figure 4. TEM images of the silica particles prepared by different amount of MPTS polycondensing with TEOS.

shell. The structure of MPTS is similar to that of APTS, except the terminal group is the mercapto but not the amino, and the three oxymethyl groups replace the three oxyethyl groups on APTS. Similar to the synthesis of silica nanoparticles using APTS, different amounts of MPTS were added to the microemulsion to form a shell on the silica nanoparticle surface. Compared to the smooth surface without MPTS (Figure 4a), a small amount of MPTS (5 μL) resulted in a rough surface of the silica nanoparticles (Figure 4b). But the roughness was not as uniform as that from APTS. When the MPTS amount increased, the particles became to adhere to each other (Figure 4c). Obviously, MPTS was not as good of a silica precursor as APTS to make the rough surface of silica nanoparticles. But the similar effect from both APTS and MPTS indicated that the one terminal end on the silane precursor plays a role in making a rough surface of silica nanoparticles.

3.5. Mechanism of Forming a Rough Surface. Based on the above results, we proposed a mechanism for the explanation of the rough surface formation on the silica cores. The molecular structures of TEOS, APTS, and MPTS are shown in Figure 5a−c. The TEOS and APTS molecules (Figure 5 a and b) have a similar chemical structure on their branches of oxyethyl groups. The difference is that the TEOS has four oxyethyl groups but the APTS has three with one terminal end of amino group. The oxyethyl groups can be hydrolyzed in the reverse microemulsion under the catalysis of ammonia. The formed hydroxyl groups can replace the oxyethyl groups and be polycondensed to a long chain containing a number of −O−Si−O− units. In the drying process, these chains cross-link and form a −O−Si−O− network by losing one molecule of C_2H_5OH or H_2O (Figure 5d). This reaction may also be accelerated by heating.[33]

The difference in the molecular structure of APTS than TEOS resulted in a different network structure of APTS (Figure 5e). The terminal amino groups could not participate in the polymerization as the other three oxyethyl groups did. As a result, the existence of the terminal amino group of APTS provided its network with more defective sites compared with the TEOS network. With the departure of C_2H_5OH and H_2O, the unperfected network collapsed and sunk. The produced nanoparticles were scaled down to smaller sizes and became the loose skeletons. Thus, the formation of the loose layer and the rough surface derived from the defects of APTS molecules. The MPTS has a similar terminal group on its molecular structure, and thus produced the silica nanoparticles with a rough surface as well.

3.6. Determination of the Amount of Amino Groups on the Rough Surface of the Nanoparticles. As described in Section 3.1, based on the BET measurement, the rough surface provided a larger surface area than the smooth one. Usually, the purpose of having a large surface area is to provide more reactive groups on the nanoparticles. Thus, we tested the available amino groups on the rough surface of the silica nanoparticles. The nanoparticle with the roughest surface, which was made from 50 μL of APTS, was chosen for this test.

The traditional acid−base titration was employed for the determination of the amino groups on the nanoparticles. The amino groups acted as the weak base. The pH value of a 0.275 mg/mL nanoparticle solution was 9.30. To accurately conduct the titration, we first adjusted the pH of this nanoparticle solution to a more basic value of 11.50 using 1.0 mL of NaOH (99.473 mmol/L). At such a condition, the amino groups existed in the form of $-NH_2$ only. In this case, the solution was composed of two bases: a strong base (excessive NaOH) and a weak base ($-NH_2$ groups on the nanoparticles). Figure 6 shows the titration curve of the acid−base reaction. At the beginning, the pH value decreased slowly in the range of 11.50−9.05 where the free OH^- from NaOH was neutralized by the HCl. Then, the pH value reduced much quickly in the range of 9.05−7.88 followed by a plateau. Afterward, a small amount of HCl solution (only 2 μL) caused the pH value reduced suddenly. The equilibrium process took about half an hour because the reaction of the weak base of amino group with H^+ ($-NH_2 + H^+ \rightarrow -NH_3^+$) was quite slow. After all the $-NH_2$ was converted to $-NH_3^+$, the pH values strongly depended on the excessive HCl. We observed a second sharp decrease at the pH range of 7.20−3.50. According to the volume consumption of HCl (about 215 μL, from 853 to 1068 μL) by $-NH_2$, the amount of amino groups was calculated to be 4.05 μmol/mg of particles. On the basis of the amount of APTS we added in the reverse microemulsion, we calculated that more than 84.0% of APTS was hydrolyzed and formed the network structure of the silica shell.

3.7. Dissociation Constant of the Amino Groups on the Silica Nanoparticles. The reactivity of the amino groups on the nanoparticles was characterized by measuring its dissociation constant. The equilibrium of amino groups in water is as below

$$-NH_2 + H_2O \leftrightarrow -NH_3^+ + OH^-$$

When reached the equilibrium, the pH of the nanoparticle solution was 9.30. On the basis of the result in Figure 6, the amounts of $-NH_3^+$ and $-NH_2$ on the silica nanoparticles were determined. The amount of $-NH_3^+$ was calculated based on the amount of NaOH used for converting $-NH_3^+$ to $-NH_2$. At the beginning, 99.4 μmol of NaOH (1.0 mL, 0.0994 ± 0.0003 M) was added. During the titration, a total of 88.7 μmol HCl (853 μL, 0.104 ± 0.001 M) was used to neutralize OH^-. The difference of 10.7 μmol OH^- was used to neutralize $-NH_3^+$ in the nanoparticle aqueous solution. Therefore, the concentration of $-NH_3^+$ was 0.535 mM and the concentration of -NH_2 was 0.578 mM. The dissociation constant of the amino groups on

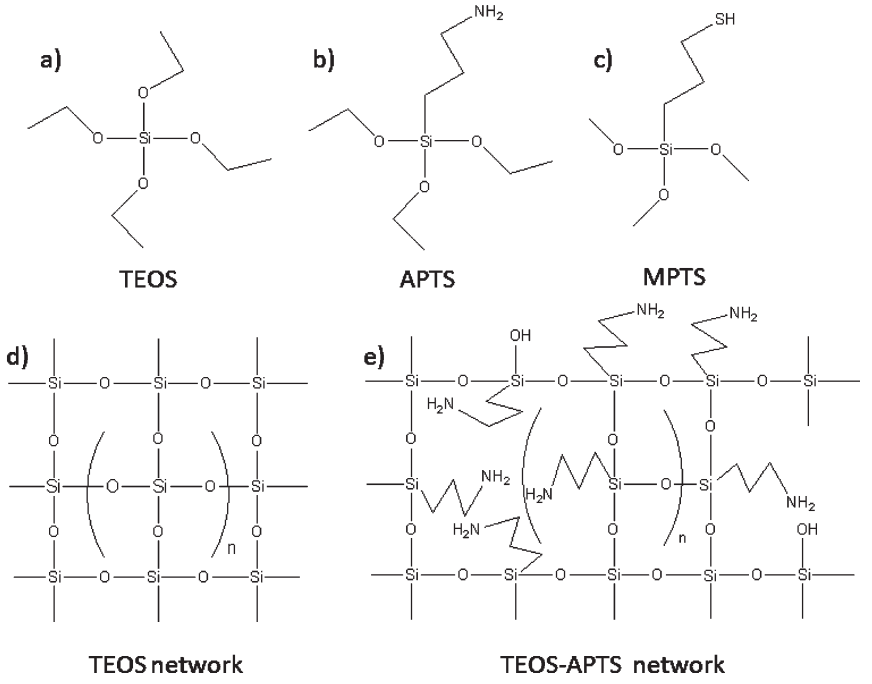

Figure 5. Molecular structures of (a) TEOS, (b) APTS, and (c) MPTS. (d, e) Schematic drawings of the networks of TEOS and TEOS-APTS after the polymerization.

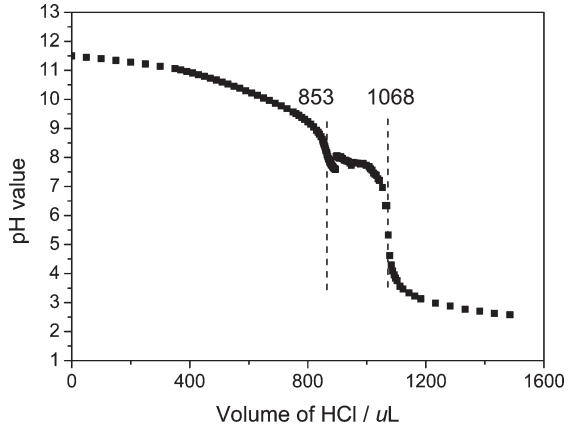

Figure 6. Titration curve of the silica nanoparticle solution by HCl (~0.1 M).

the silica particles can be expressed in the form of pK_a. Thus, $pK_a = pH + \log[-NH_3^+]/[-NH_2] = 9.30 + \log 0.929 = 9.27$.

3.8. Application of the Nanoparticle with a Rough Surface for Chemical Binding of an NIR Dye. Silica nanoparticles have a wide variety of applications after the effective surface functionalization. In our present study, the produced rough surface provided silica nanoparticles with a large number of surface amino groups. The amino groups are highly valuable functional groups that can react with some important chemicals in the applications of the silica nanoparticles. For example, the amino can react with isothiocyanate groups under mildly alkaline conditions; it can also react with α-carboxyl groups to form an amide bond.

To demonstrate the potential applications of the developed silica nanoparticles with a rough surface, we explored these nanoparticles for concentration of an NIR active dye, NIR 797 isothiocyanate, and further to prepare the NIR−active silica nanocomplex. The nanocomplex can be an excellent NIR labeling reagent for detection of biological samples since the NIR region is a favorable bioanalysis window. The reaction between the NIR 797 isothiocyanate and the amino group is as below:

$$R{-}N{=}C{=}S + NH_2{-}(CH_2)_3{-}Si{-}(OC_2H_5)_3$$

$$\rightarrow R{-}NH{-}(S{=})C{-}NH{-}(CH_2)_3{-}Si{-}(OC_2H_5)_3$$

$$R = \text{NIR 797 chromophore}$$

After linking with NIR 797 isothiocyanate, the color of the silica particles changed to green (Figure 7a). UV−vis spectra of the NIR dye-linked silica nanoparticles are shown in Figure 7b. NIR 797 isothiocyanate has two typical absorption bands at ~710 and ~820 nm. We plotted the concentration vs the integral area of NIR 797 isothiocyanate as a calibration curve (Figure 7c). The calibration equation was obtained as $y = 0.098(\pm 0.456)x$, while $R = 0.995$ ($n = 8$). The integral area indicated the amount of the NIR dye. Figure 7d shows the integral area of the absorption spectra corresponding to Figure 7b, which reflected the adsorption ability of silica particles with different roughness. Surprisingly, the roughest surface of silica nanoparticles did not show the strongest adsorption of the linked dye molecules. Rather, the 30 μL APTS silica nanoparticles presented the strongest adsorption ability The amount of NIR dye on the 40 and 50 μL APTS particles decreased slightly, but they still possessed the strong adsorption ability for NIR dye.

3.9. Application of the Developed Nanoparticles for Supramolecular Adsorption of Au Nanoparticles. The rough surface provided silica nanoparticles with a larger surface area. The above application demonstrated its application for chemical binding of targets. Furthermore, we tested its ability on the supramolecular adsorption of targets by capturing gold nanoparticles onto the silica nanoparticles. The Au nanoparticles of 4 ± 1 nm

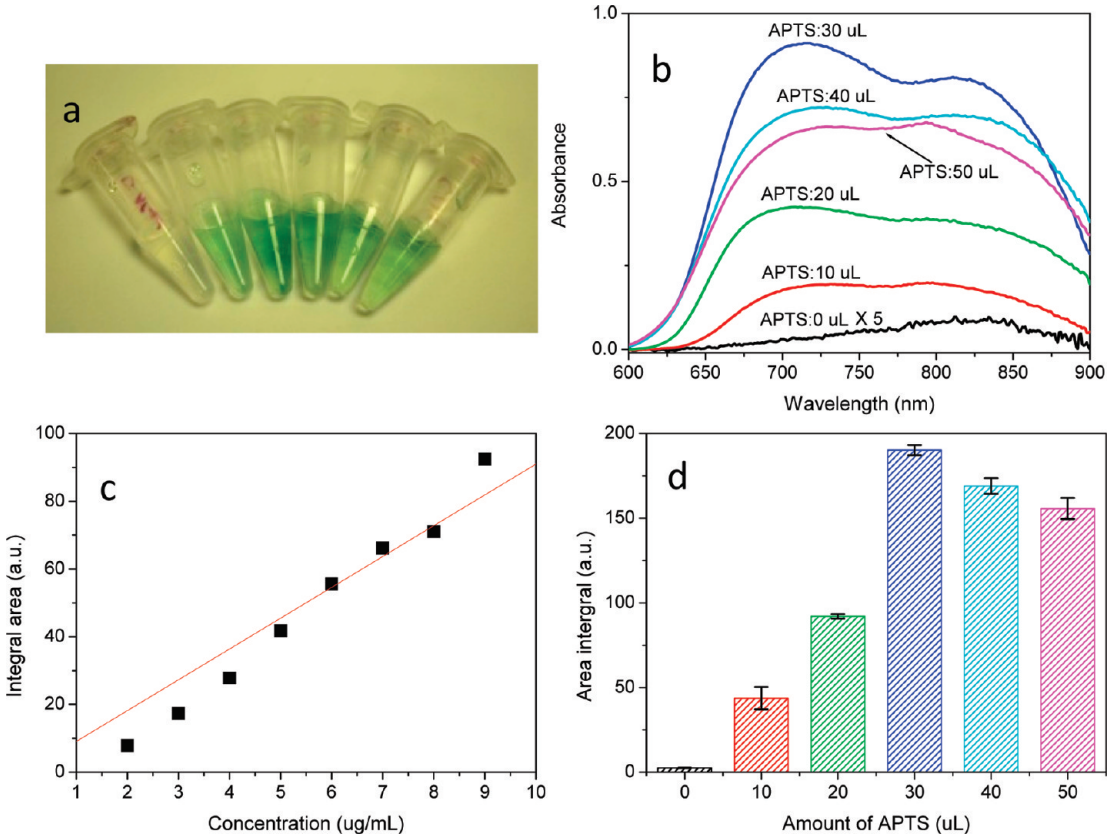

Figure 7. (a) Silica−NIR dye nanocomplex suspended solutions. Left to right: 0, 10, 20, 30, 40, and 50 μL APTS were used for synthesis of the silica nanoparticles. (b) UV−vis spectra of silica−NIR 797 isothiocyanate nanocomplexes (containing 0.33 mg/mL of silica nanoparticles). (c) Calibration curve of the integral area of the absorption spectra vs the concentration of NIR dye. (d) Comparison of the adsorption amounts of NIR dye on different silica nanoparticles.

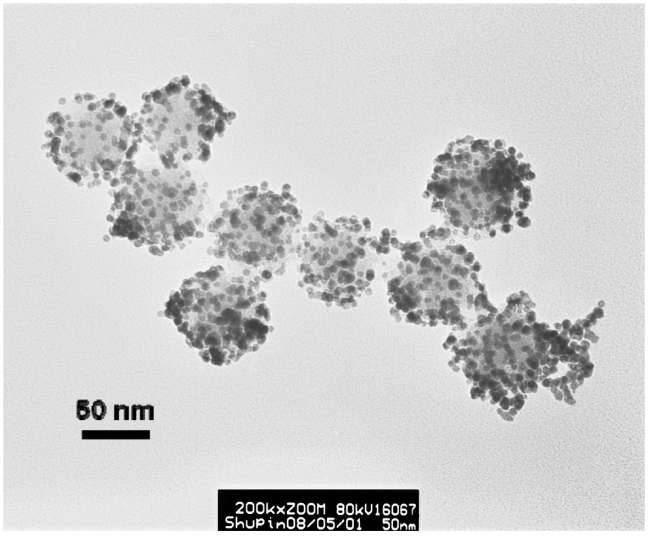

Figure 8. TEM image of the silica−Au satellitic nanocomplexes.

in diameter were synthesized, and then were added into the silica nanoparticle solution. After 5 min, the gold nanoparticles were easily captured by the silica particles and formed silica−Au satellitic nanocomplexes due to the strong interaction between Au and amino groups.[34] The nanocomplex showed good dispersion on the TEM image (Figure 8). They also presented an excellent stability relative to the gold colloids. The nanocomplexes can be easily resuspended in the aqueous solution even after they were centrifuged several times. The improved stability is important for applications of the gold nanoparticles in various fields. Thus, the nanoparticles with a rough surface can be used as an effective solid-supporting matrix for carrying and dispersion of very small metal nanoparticles.

4. CONCLUSIONS

Controlling the architecture at the nanoscale has been a challenge in the field of nanoscience and nanotechnology. In present work, we have developed a universal method to construct a rough silica layer on the spherical silica nanoparticles. The level of the surface roughness can be successfully controlled by adjusting the amount of functional silane precursors. Using the acid−base titration method, the coverage of amino groups on the silica nanoparticle has been determined to be 4.05 μmol of amino groups/mg silica particles. These silica nanoparticles were an excellent solid-supporting carrier for containing NIR dye molecules and adsorption of small gold nanoparticles. These rough surface silica nanoparticles could be a promising nano carrier for entrapping not only the small organic molecules but also the functional nanoparticles.

■ ASSOCIATED CONTENT

Ⓢ Supporting Information. BET analyses; DLS results. This material is available free of charge via the Internet at http://pubs.acs.org.

AUTHOR INFORMATION

Corresponding Author
*E-mail: jzhao@chem.und.edu. Tel: 701-777-3610.

ACKNOWLEDGMENT

This work is partially supported by the National Science Foundation Grant CHE-0911472 and EPS-0814442, North Dakota EPSCoR Seed Grant. We thank the Imaging Center at the Medical School of University of North Dakota for the convenience of using the electronic microscopes.

REFERENCES

(1) Halas, N. J. *ACS Nano* **2008**, *2*, 179.
(2) Zhao, X.; Hilliard, L. R.; Wang, K.; Tan, W. In *Encyclopedia of Nanoscience and Nanotechnology*; Nalwa, H. S., Ed.; American Scientific Publishers: Stevenson Ranch, CA, 2004.
(3) Wang, L.; Wang, K. M.; Santra, S.; Zhao, X. J.; Hilliard, L. R.; Smith, J. E.; Wu, Y. R.; Tan, W. H. *Anal. Chem.* **2006**, *78*, 646.
(4) Jin, Y.; Kannan, S.; Wu, M.; Zhao, J. X. *Chem. Res. Toxicol.* **2007**, *20*, 1126.
(5) Xu, S.; Hartvickson, S.; Zhao, J. X. *Langmuir* **2008**, *24*, 7492.
(6) Jin, Y.; Li, A.; John, C. L.; Hazelton, S. G.; Liang, S.; Selid, P. D.; Pierce, D. T.; Zhao, J. X. *Coord. Chem. Rev.* **2009**, *253*, 2998.
(7) Santra, S; Bagwe, R. P.; Dutta, D.; Stanley, J. T.; Tan, W.; Moudgil, B. M.; Mericle, R. A. *Adv. Mater.* **2005**, *17*, 2165.
(8) Santra, S.; Wang, K.; Tapec, R.; Tan, W. H. *J. Biomed. Opt.* **2001**, *6*, 1.
(9) Santra, S.; Zhang, P.; Wang, K.; Tapec, R.; Tan, W. H. *Anal. Chem.* **2001**, *73*, 4988.
(10) Jin, Y.; Lohstreter, S.; Pierce, D. T.; Parisien, J.; Wu, M.; Hall, C., III; Zhao, J. X. *Chem. Mater.* **2008**, *20*, 4411.
(11) Santra, S.; Zhang, P.; Wang, K. M.; Tapec, R.; Tan, W. H. *Anal. Chem.* **2001**, *73*, 4988.
(12) Zhao, X.; Dytocio, R. T.; Tan, W. H. *J. Am. Chem. Soc.* **2003**, *125*, 11474.
(13) He, X. X.; Wang, K. M.; Tan, W. H.; Liu, B.; Lin, X.; He, C. M.; Li, D.; Huang, S. S.; Li, J. *J. Am. Chem. Soc.* **2003**, *125*, 7168.
(14) Bromley, S. T.; Moreira, I. D. R.; Neyman, K. M.; Illas, F. *Chem. Soc. Rev.* **2009**, *38* (9), 2657–2670.
(15) Stromme, M.; Brohede, U.; Atluri, R.; Garcia-Bennett, A. E. *Interdiscip. Rev. Nanomed. Nanobiotechnol.* **2009**, *1* (1), 140–148.
(16) Piao, Y.; Burns, A.; Kim, J.; Wiesner, U.; Hyeon, Y. *Adv. Funct. Mater.* **2008**, *18* (23), 3745–3758.
(17) Tallury, P.; Payton, K.; Santra, S. *Nanomedicine* **2008**, *3* (4), 579–592.
(18) Stöber, W.; Fink, A. *J. Colloid Interface Sci.* **1968**, *26*, 62.
(19) Bagwe, R. P.; Yang, C. Y.; Hilliard, L. R.; Tan, W. H. *Langmuir* **2004**, *20*, 8336.
(20) George, T. F.; Jelski, D. A. *J. Phys. Chem.* **1987**, *91*, 3779.
(21) Beysens, D. A.; Narhe, R. D. *Langmuir* **2007**, *23*, 6486.
(22) Marmur, A. *Langmuir* **2003**, *19*, 8343.
(23) You, Y.-Z.; Kalebaila, K. K.; Brock, S. L.; Oupický, D. *Chem. Mater.* **2008**, *20*, 3354.
(24) Roy, I.; Ohulchanskyy, T. Y.; Bharali, D. J.; Pudavar, H. E.; Mistretta, R. A.; Kaur, N.; Prasad, P. N. *Proc. Natl. Acad. Sci. U.S.A.* **2005**, *102*, 279.
(25) Yang, J.; Lee, J.; Kang, J.; Lee, K.; Suh, J.-S.; Yoon, H.-G.; Huh, Y.-M.; Haam, S. *Langmuir* **2008**, *24*, 3417.
(26) Saffarian, H. M.; Srinivasan, R. *J. Phys. Chem. B* **2002**, *106*, 7042.
(27) Liang, S.; Hartvickson, S.; Kozliak, E.; Zhao, J. X. *J. Phys. Chem. C* **2009**, *113*, 19046.
(28) Haynes, C. L.; VanDuyne, R. P. *Nano Lett.* **2003**, *3*, 939.
(29) Felidj, N.; Aubard, J.; Levi, G.; Krenn, J. R.; Hohenau, A.; Schider, G.; Leitner, A.; Aussenegg, F. R. *Appl. Phys. Lett.* **2003**, *82*, 3095.
(30) Black, C. T. *ACS Nano* **2007**, *1*, 147.
(31) Kumar, R.; Roy, I.; Ohulchanskyy, T. Y.; Goswami, L. N.; Bonoiu, A. C.; Bergey, E. J.; Tramposch, K. M.; Maitra, A.; Prasad, P. N. *ACS Nano* **2008**, *2*, 449.
(32) In *Bioconjugate Techniques*; Hermanson, G. T., Ed.; Academic Press: San Diego, CA, 1996.
(33) Ek, S.; Iiskola, E. I.; Niinistö, L.; Vaittinen, J.; Pakkanen, T. T.; Keränen, J.; Auroux, A. *Langmuir* **2003**, *19*, 10601.
(34) Osterloh, F.; Hiramatsu, H.; Porter, R.; Guo, T. *Langmuir* **2004**, *20*, 5553.